Crystallization Kinetics of Compatibilized Blends of a Liquid Crystalline Polymer with Polypropylene

S. C. TJONG, S. X. CHEN, R. K. Y. LI

Department of Physics and Materials Science, City University of Hong Kong, 83 Tat Chee Avenue, Kowloon, Hong Kong

Received 10 May 1996; accepted 20 October 1996

ABSTRACT: Blends of a maleic anhydride-grafted polypropylene (m-PP) and a liquid crystalline polymer (LCP) based on a copolyester of hydroxynapthoic acid and hydroxybenzoic acid were fabricated. The morphology and isothermal and nonisothermal crystallization kinetics behavior of the m-PP copolymer and m-PP/LCP blends were investigated using polarizing optical microscopy, depolarized light intensity, and differential scanning calorimetry. A polarizing optical micrograph revealed that the m-PP is very effective to promote a finer dispersion of the LCP phase in the PP matrix. Consequently, the LCP domains or fibrils acted as potential sites for the spherulite nucleation. The isothermal kinetics measurements also indicated that the rate of crystallization is enhanced in the maleated PP/LCP blends which exhibit transcrystallinity. In general, the nonisothermal kinetics results were in good agreement with those obtained from the isothermal kinetics measurements. © 1997 John Wiley & Sons, Inc. J Appl Polym Sci **64:** 707–715, 1997

Key words: liquid crystalline polymer; compatibilizer; polypropylene; morphology; crystallization kinetics

INTRODUCTION

Thermotropic liquid crystalline polymers (LCPs) have been the subject of active research interest in recent years because of their potential use for high strength, high modulus, and chemical-resistant materials. LCPs are composed of long-chain rodlike molecules that exhibit an ordered state in the melt. The orientation of the rodlike molecules during extensional flow permits significant reinforcement in thermoplastics. The self-orienting fibrous structure then functions as a reinforcing element. The composite made in this way is termed an *in situ* composite.

Reinforcement of thermoplastics with several LCPs has been studied by several researchers extensively.[1–11] In most cases, LCPs are incompatible with thermoplastic polymers because the melt of the former is in an anisotropic state and that of the latter is isotropic. Thus, a two-phase morphology is typically formed in the binary blend. Morphologies ranging from spherical droplets to long fibrils have been observed in incompatible LCP/thermoplastic blends. The morphology of the blend is of primary importance as it directly affects the final mechanical properties. For the effective transfer of stress between the reinforcement and the matrix, the LCP domains must exhibit fine fibrils with large aspect ratios.

It is generally known that the incompatibility between the matrix polymers and reinforcing LCPs leads to poor interfacial adhesion. The reinforcing effect is substantially smaller than that obtained from the compatible blends. Recently, much attention has been paid to the possibility of modifying the interfacial adhesion of PP/LCP blends by the addition of a third component which

Correspondence to: S. C. Tjong.
Contract grant sponsor: City University of Hong Kong.
Contract grant number: 7000-502.
© 1997 John Wiley & Sons, Inc. CCC 0021-8995/97/040707-09

acts as a compatibilizer.[12–14] The compatibilizing agents used by these workers were mostly polyolefins functionalized with maleic anhydride (MA).[11–14] The functional groups of the MA interact with the amide groups of LCP, giving rise to strong links between the two phases. Consequently, compatibilization leads to a reduction in interfacial tensions, thereby promoting a finer dispersion and more uniform distribution of the LCP phase within the matrix.[13,14] The morphology, impact, static, and dynamic mechanical properties of PP/LCP blends were investigated previously. However, less information is available on the effect of MA on the crystallization behavior of the PP and PP/LCP blends. The isothermal[15–18] and nonisothermal[19–22] crystallization kinetics of pure PP were reported in the literature. This work was aimed to investigate the crystallization kinetics behavior of the compatibilized and noncompatibilized PP/LCP blends using depolarized light intensity and differential scanning calorimetry (DSC) measurements. The understanding of the nonisothermal melt-crystallization behavior of PP/LCP blends leads to a better control of the final properties of the polymer blends, generally processed under nonisothermal conditions.

EXPERIMENTAL

Material

The thermotropic liquid crystalline polymer (LCP) used in this work is Vectra A950 produced by the Hoechst Celanese Co. Vectra A950 is a wholly aromatic copolyester consisting of 25 mol % of 2,6-hydroxynaphthoic acid (HNA) and 75 mol % of *p*-hydroxybenzoic acid (HBA). The PP matrix is a commercial product of the Himont Co. (Pro-fax 6331) with a melt flow index of 12. The compatibilizer is a maleic anhydride (MA) supplied by Fluka Chemie, whereas the dicumyl peroxide produced by Aldrich Chemical Co. is used for the maleation of the PP.

Blending and Processing

Maleation was carried out by feeding a mixture of the PP pellets, 6 wt % MA, and 0.3 wt % dicumyl peroxide in a twin-screw Brabender operated at 200°C. The maleated PP is then pelletized and is designated as m-PP in this study. Both polymer pellets of m-PP and LCP were dried in an oven operated at 70 and 150°C for 24 h, respectively. The pellets containing 5, 10, 20, 30, and 40 wt % LCP were tumbled together in a box before extrusion. The compatibilized PP/LCP blends were then prepared in Brabender with an attached slit die of 50×0.5 mm^2. The barrel temperature from the root to the die was maintained at 290, 295, 295, and 290°C, respectively. A similar procedure was adopted to fabricate the noncompatibilized PP/LCP blends.

Characterization

Fourier transform infrared spectroscopy (FTIR) was used to characterize the changes in the chemical structure of the PP matrix after maleation. Thin-film specimens with a thickness of about 40 μm were prepared from the melt, and the FTIR analyses were made with a Perkin-Elmer 16 PC spectrometer.

The crystalline morphology of both noncompatibilized and compatibilized PP/LCP blends was observed with a polarizing optical microscope (Model Olympus BH-2). In the process, thin spec-

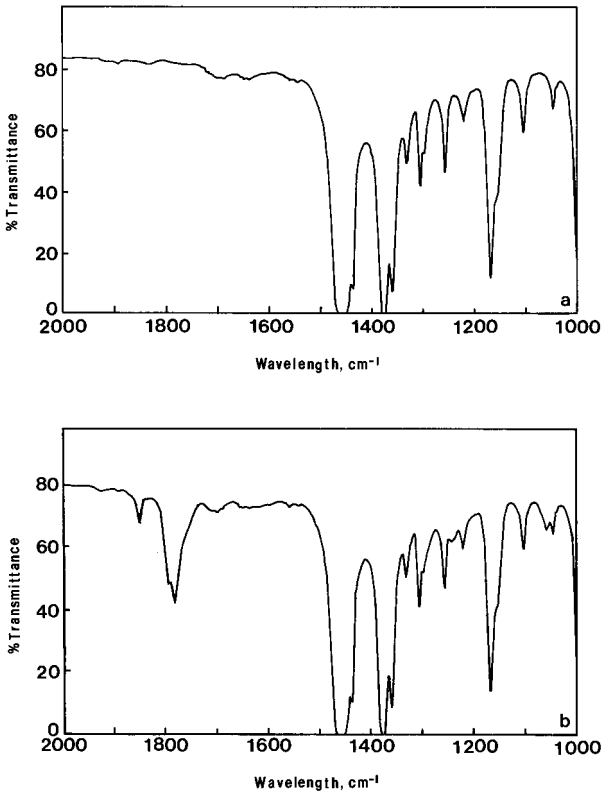

Figure 1 FTIR spectra of (a) pure and (b) maleated PP specimens.

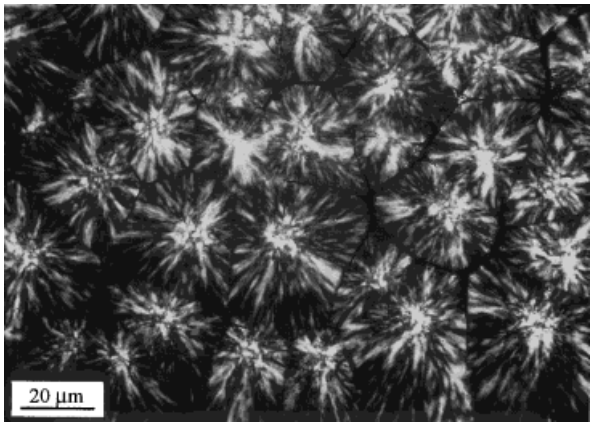

Figure 2 POM micrograph showing the spherulitic morphology of the m-PP copolymer crystallized at 115°C.

imens were initially heated to 300°C. They were held at this temperature for 10 min to assure their complete melting. The specimens were allowed to cool down from 300°C to room temperature slowly.

Kinetics Measurements

The isothermal crystallization kinetics of noncompatibilized and compatibilized PP/LCP blends

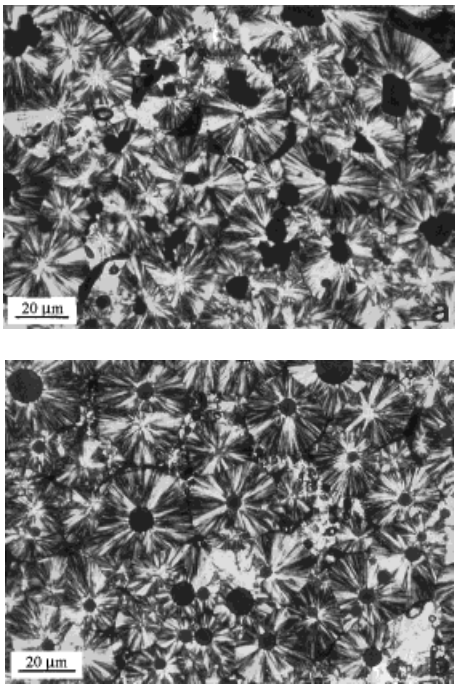

Figure 3 POM micrographs showing the spherulitic morphology of (a) PP/10% LCP and (b) m-PP/10% LCP blends.

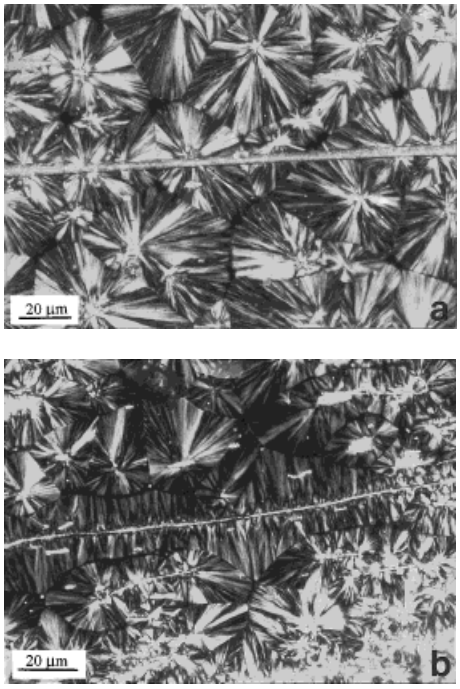

Figure 4 POM micrographs showing (a) the spherulitic morphology of the PP/10% LCP blend and (b) the transcrystalline spherulitic feature of the m-PP/10% LCP blend. The micrographs were taken by shearing the melt prior to crystallization.

was investigated by measuring the intensity of transmitted light from specimens placed between crossed polaroids. In other words, the intensity of depolarized light passing through the specimens during isothermal treatments at temperature in the range 110–123°C was recorded. The specimens were placed between two glass slides, and they were heated to 300°C in the hot stage for 1 min, then cooled rapidly to the crystallization temperature.

A Perkin-Elmer differential scanning calorimeter, Model DSC-7, was employed to study the nonisothermal crystallization kinetics of the polymer blends. Indium and zinc standards were used for temperature calibration. In the test, the specimens were initially heated to 300°C, held 1 min at this temperature, and then cooled to 50°C at various predetermined rates. The rates employed were 10, 15, 20, 25, 30, and 40°C/min, respectively.

RESULTS AND DISCUSSION

General Behavior

Figure 1(a) and (b) shows the FTIR spectra of pure PP and m-PP, respectively. It can be seen

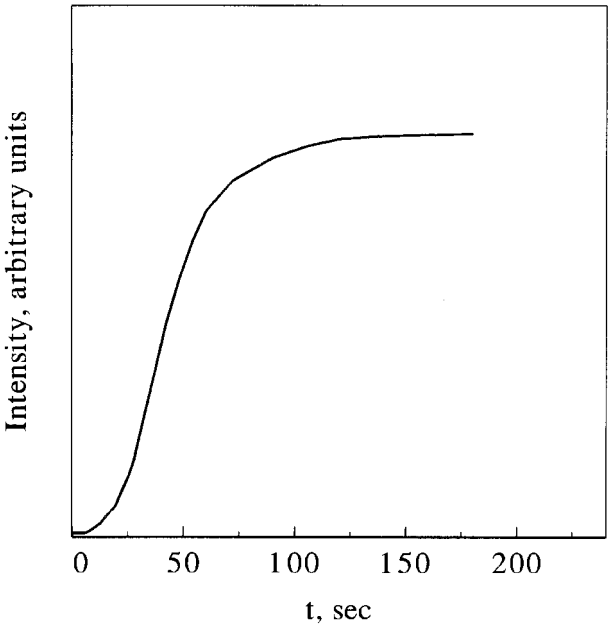

Figure 5 Intensity of depolarized light during isothermal crystallization at 115°C vs. time.

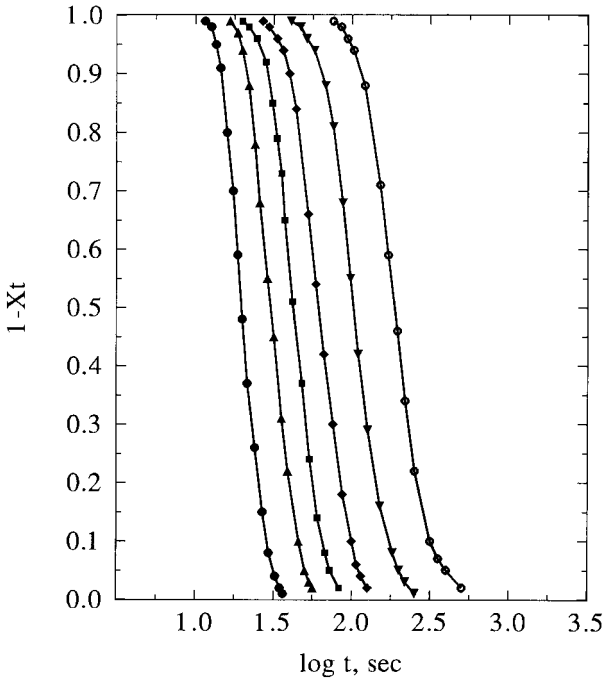

Figure 6 Plots of $(1 - X_t)$ vs. $\log t$ of the m-PP copolymer during isothermal crystallization at different temperatures: (●) 110°C; (▲) 113°C; (■) 115°C; (♦) 117°C; (▼) 120°C; (○) 123°C.

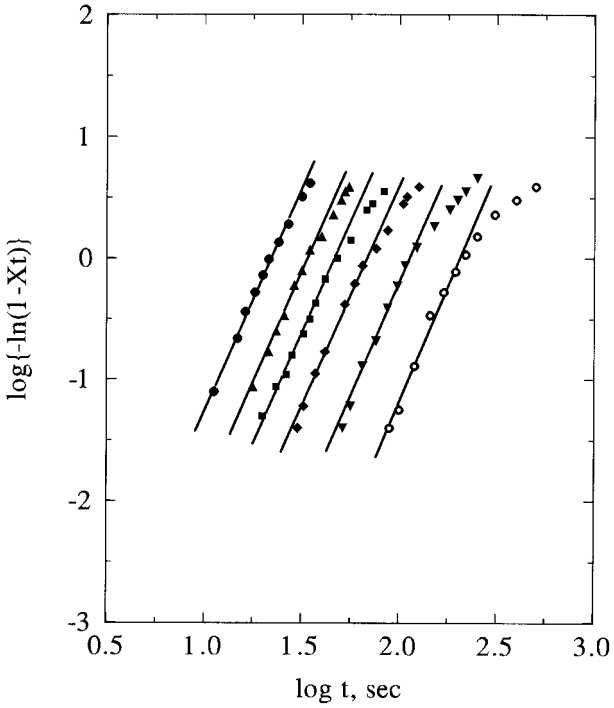

Figure 7 Plots of $\log[-\ln(1 - X_t)]$ vs. $\log t$ of the m-PP copolymer during isothermal crystallization at different temperatures: (●) 110°C; (▲) 113°C; (■) 115°C; (♦) 117°C; (▼) 120°C; (○) 123°C.

that the m-PP exhibits a characteristic vibrational band at 1790 cm^{-1} which corresponds to the carbonyl groups conjugated with methylene sequences.[23] It is well known that MA exhibits a strong carbonyl absorption peak at 1788 cm^{-1}. Thus, the FTIR spectra indicate that MA is efficiently grafted to the PP specimen.

Figure 2 shows a POM micrograph of m-PP crystallized at 115°C for 1 h. It is apparent from this micrograph that the spherulitic morphology is similar to that of neat PP, i.e., it exhibits a typical Maltese cross extinction pattern. However, the addition of a second LCP phase can yield

Table I Kinetic Parameters for Isothermal Crystallization of m-PP

T_c (°C)	$t_{1/2}$ (s)	n	k (s^{-1})
110	20	4	4.33×10^{-6}
113	30	4	8.56×10^{-7}
115	42	4	2.23×10^{-7}
117	60	4	5.35×10^{-8}
120	100	4	6.93×10^{-9}
123	182	4	6.32×10^{-10}

Table II Kinetic Parameters for Isothermal Crystallization of PP and Its Blends at 115°C

PP/LCP	$t_{1/2}$ (s)	n	k (s^{-1})
100/0	52	4	9.48×10^{-8}
95/5	46	3.7	4.88×10^{-7}
90/10	50	3.8	2.42×10^{-7}
80/20	48	3.8	2.83×10^{-7}
70/30	49	3.8	2.61×10^{-7}
60/40	49	3.8	2.61×10^{-7}

many additional surface sites for the nucleation of spherulites. Figure 3(a) and (b) shows the spherulitic morphology of PP/10% LCP and m-PP/10% LCP blends, respectively. It is evident that the LCP domains act as nuclei for the nucleation of the spherulites. Also, these spherulites tend to grow radially from the center outward. The size of the spherulites of m-PP/10% LCP is considerably smaller than that of the m-PP specimen. Moreover, it can be seen that the LCP phase domains of the m-PP/10% LCP blend are relatively smaller than those of the PP/10% LCP blend. This implies that the MA addition is very effective to promote a finer dispersion of the LCP phase.

The LCP fibrils can be observed in the blends when the glass slides containing the molten polymer specimens were initially sheared. Figure 4(a) and (b) shows the POM micrographs of PP/10% LCP and m-PP/10% LCP specimens containing LCP fibrils. It is apparent that the fine LCP fibrils of m-PP/10% LCP induce a very dense nucleation and growth of the spherulites on its surface, i.e., transcrystalline morphology. For the region further away from the LCP fibrils, the bulk-crystallization process prevails. Transcrystallinity is also observed for the m-PP/LCP blends containing LCP content above 10 wt %. The transcrystalline

Table III Kinetic Parameters for Isothermal Crystallization of m-PP and Its Blends at 115°C

m-PP/LCP	$t_{1/2}$ (s)	n	k (s^{-1})
100/0	42	4	2.23×10^{-7}
95/5	36	3.8	8.45×10^{-7}
90/10	40	3.3	3.57×10^{-6}
80/20	39	3.2	5.63×10^{-6}
70/30	39	3.2	5.63×10^{-6}
60/40	39	3.2	5.63×10^{-6}

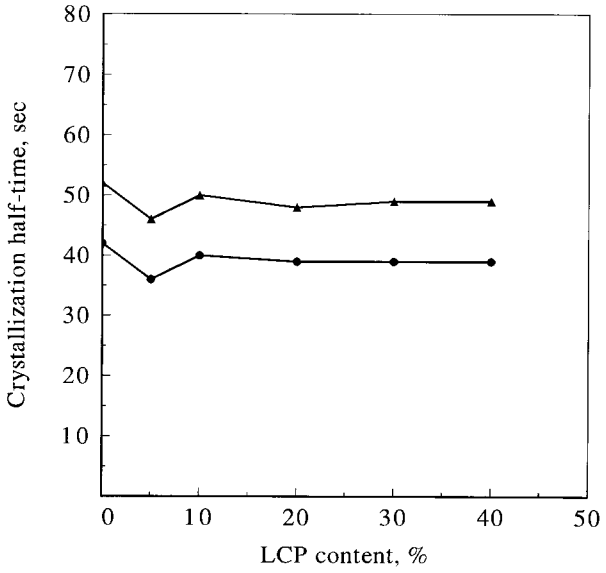

Figure 8 Half-time of crystallization vs. LCP content for PP/LCP and m-PP/LCP blends: (●) m-PP copolymers; (▲) PP homopolymer.

growth observed in the m-PP/LCP blend is considered analogous to that observed in the carbon fiber-reinforced PPS thin film. Desio and Rebenfeld[24] reported that the rate of crystallization was enhanced in the PPS film/carbon fiber composites which exhibited transcrystallinity. However, the LCP fibrils in PP/10% LCP blend generally do not induce transcrystallinity [Fig. 4(a)].

Isothermal Melt Crystallization

Figure 5 shows a typical crystallization isotherm of m-PP at 115°C obtained from the depolarized light intensity measurement. The crystallization isotherm can be analyzed in terms of the Avrami equation

$$1 - X_t = I_\infty - I_t/I_\infty - I_0 = \exp(-kt^n) \quad (1)$$

where X_t is the fraction of material crystallized after time t; I_t, the transmitted intensity at time t; and I_0 and I_∞, the values of I_t at $t = 0$ and $t = \infty$, respectively. The parameters k and n are related to the rate and mechanism of crystallization.

Figure 6(a) shows the plots of $(1 - X_t)$ vs. log t of the m-PP specimen at various crystallization temperatures (T_c). It is apparent from this figure that the fraction of untransformed (amorphous) material has an inverted "S" shape dependence on the logarithm of time. The Avrami exponent n

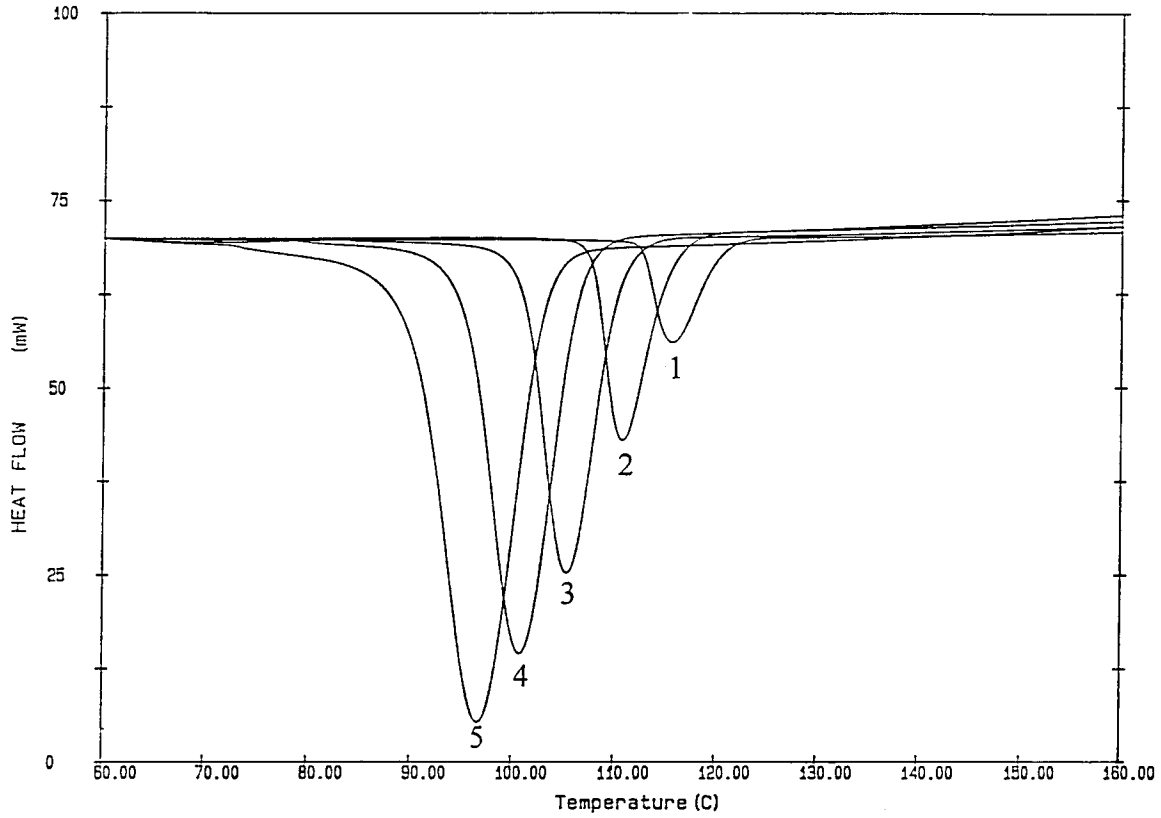

Figure 9 DSC cooling traces of the m-PP copolymer during nonisothermal crystallization at different cooling rates: (1) 10°C/min; (2) 15°C/min; (3) 20°C/min; (4) 30°C/min; (5) 40°C/min.

can be obtained from the double logarithmic form of the Avrami equation

$$\log[-\ln(1 - X_t)] = \log k + n \log t \qquad (2)$$

Figure 7 shows the plots of $\log[-\ln(1 - X_t)]$ vs. $\log t$ for the m-PP specimen at various T_c. Obviously, such plots yield several straight lines with a slope of 4 over a wide range of T_c. The parameter k can be determined from eq. (1):

$$k = \ln 2/(t_{1/2})^n \qquad (3)$$

where $t_{1/2}$ is the half-time of crystallization, i.e., the time at which the depolarized light intensity reaches one-half of its final value. Tables I–III list the isothermal crystallization kinetics parameters for the m-PP copolymer, PP/LCP, and m-PP/LCP blends, respectively.

According to the Avrami theory, the exponent n depends on the geometry of crystal growth and on the type of nucleation. Athermal nucleation and spherulitic growth lead to an Avrami exponent of 3, whereas thermal nucleation and spherulitic growth, to a value of 4.[25] Based on the experimental results as tabulated in the above tables, it is obvious that both the PP homopolymer and m-PP copolymer exhibit an Avrami exponent of 4. It implies that grafting the PP with MA has no effect on the spherulitic nucleation and growth. However, the incorporation of the LCP phase into the homopolymer matrix leads to a decrease in the exponent n, particularly for the m-PP/LCP blends. This decrease is due to that the LCP domains in the m-PP/LCP blends act as the heterogeneous nucleation sites, followed by three-dimensional spherulitic growth. Moreover, it is noted that the half-time of crystallization of the PP/LCP and m-PP/LCP blends is considerably smaller than that of their corresponding homo- and copolymers. Figure 8 shows the variation of $t_{1/2}$ with the LCP content for both PP/LCP and m-PP/LCP blends. The m-PP/LCP blends have a smaller $t_{1/2}$ value than that of the PP/LCP blends.

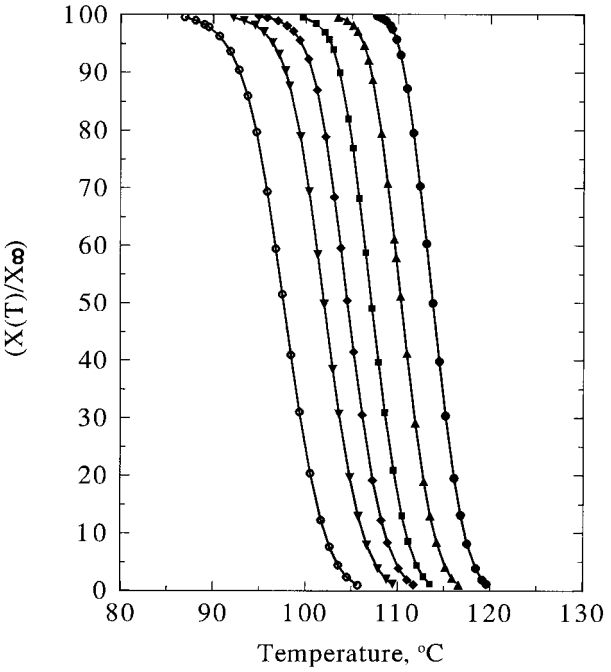

Figure 10 Plots of $[X(T)/X\infty]$ vs. T of the m-PP copolymer during nonisothermal crystallization at different cooling rates: (●) 10°C/min; (▲) 15°C/min; (■) 20°C/min; (♦) 25°C/min; (▼) 30°C/min; (○) 40°C/min.

On the basis of these results, it appears that the LCP-reinforced systems crystallize faster than does the homopolymer, and the mPP/LCP blends crystallize faster than do the uncompatibilized PP/LCP blends. In other words, the rate of crystallization is enhanced in the m-PP/LCP blends which exhibit transcrystallinity. Moreover, the maleated PP tends to improve the interfacial adhesion and to promote a more uniform of LCP distribution in the m-PP/LCP blends.

Nonisothermal Melt Crystallization

The nonisothermal crystallization of the PP/LCP and m-PP/LCP blends was carried out using DSC measurements. Ozawa[26] extended the isothermal kinetic crystallization to the nonisothermal case of a controlled cooling rate. From the Evans model,[27] Ozawa derived the following relationship:

$$X(T)/X\infty = 1 - \exp[-k(T)/c^n] \qquad (4)$$

where $X(T)$ is the crystallinity attained at temperature T; $X\infty$, the crystallinity at the termination of the crystallization process; $k(T)$, a constant for a given cooling rate; c, a cooling rate; and n, the Ozawa index. This index is somewhat similar to the Avrami exponent, and it depends on the type of nucleation and the growth dimensions. The double logarithmic form of the Ozawa equation exhibits the following relationship:

$$\ln\{-\ln[1 - X(T)/X\infty]\} = \ln k(T) + n \ln(1/c) \qquad (5)$$

Similarly, the plots of $\ln\{-\ln[1 - X(T)/X\infty]\}$ vs. $\ln(1/c)$ at a fixed temperature should yield a straight line. The parameters n and $k(T)$ can be determined from the slope and the intercept of the line, respectively.

Figure 9 shows typical DSC traces for the crystallization of the m-PP matrix at various cooling rates. From the DSC profiles, the transformed fraction, $X(T)/X\infty$, is calculated as a function of temperature. The variation of $X(T)/X\infty$ vs. T for the m-PP specimen at various cooling rates is shown in Figure 10. The plots of $\ln\{-\ln[1 - X(T)/X\infty]\}$ vs. $\ln(1/c)$ for the m-PP specimen at various temperatures is shown in Figure 11. Similarly, these plots yield several straight lines with

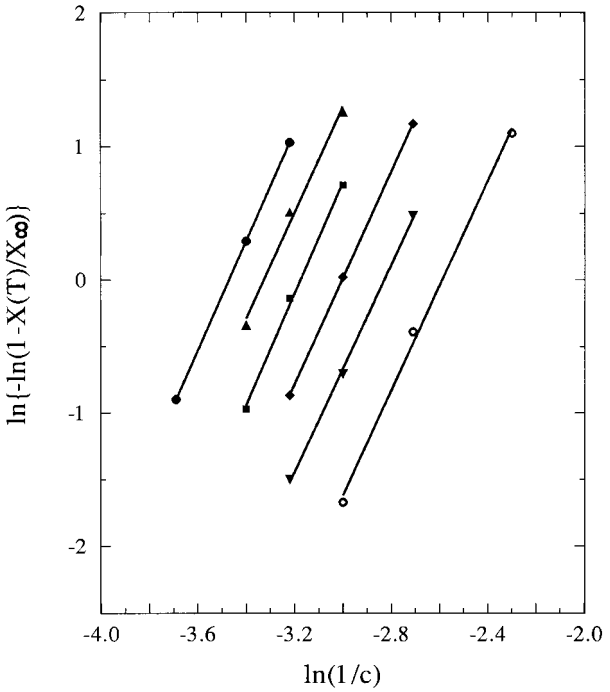

Figure 11 Plots of $\ln\{-\ln[1 - (X(T)/X\infty))]\}$ vs. $\ln(1/c)$ of the m-PP copolymer during nonisothermal crystallization at various temperatures: (●) 100°C; (▲) 102°C; (■) 104°C; (♦) 106°C; (▼) 108°C; (○) 110°C.

Table IV Kinetic Parameters for Nonisothermal Crystallization of PP and Its Blends with LCP Calculated for 105°C

PP/LCP	T_m (°C)	$T_{1/2}$ (°C)	n	X_c	k ($T_{1/2}$)
100/0	168	105	4	0.44	4.33×10^{-6}
95/5	167	106	3.7	0.48	1.07×10^{-5}
90/10	167	108	3.8	0.48	7.90×10^{-5}
80/20	166	108	3.8	0.53	7.90×10^{-5}
70/30	168	107	3.8	0.55	7.90×10^{-5}
60/40	170	108	3.8	0.61	7.90×10^{-5}

a slope of 4. At a given temperature, it appears that only three cooling rates are used in the plots of double logarithmic form of the Ozawa equation; thus, it is more appropriate to determine the parameter $k(T)$ by using the following equation:

$$k(T_{1/2}) = \ln 2/c^n \qquad (6)$$

where $T_{1/2}$ is the temperature at which 50% of the crystalline phase has been attained. The nonisothermal kinetics parameters for the PP and their blends are listed in Tables IV and V. From these tables, the degree of crystallinity (X_c) of pure PP and m-PP specimens is determined according to

$$X_c(\%) = (\Delta H_m/\Delta H_m^0) \times 100 \qquad (7)$$

where ΔH_m^0 is the heat of fusion of isotactic PP with a 100% crystalline phase (209 J/g).[28] For the PP/LCP and m-PP/LCP blends, we assume that the contribution of the LCP phase to the enthalpy of fusion is negligible.

On the basis of the nonisothermal crystallization measurements, the Ozawa exponent of PP and m-PP specimens is 4. However, the PP/LCP blends exhibit almost a constant value of 3.8, whereas the m-PP/LCP blends have an average value of 3.5. It is noted that the n value of m-PP/LCP blends tends to decrease with increasing LCP content, and the degree of crystallinity appears to increase slightly with increasing LCP content. The Ozawa exponents of the PP, m-PP, and PP/LCP blends are identical to those of the isothermal Avrami exponent, whereas the Ozawa exponent of the m-PP/LCP blends is slightly larger than that of the Avrami exponent. Generally, the results of nonisothermal kinetics measurement for both blend systems are in good agreement with those obtained from the isothermal kinetics measurements.

CONCLUSIONS

Our results indicate that the LCP phase affects the crystallization behavior of PP polymer dramatically. In general, the spherulitic size of PP tends to decrease with the LCP addition. As the LCP and PP phase are incompatible, the addition of maleic anhydride-grafted PP (m-PP) to the LCP system is observed to be very effective in promoting a finer dispersion of LCP phase in the matrix. Transcrystallinity is observed in the maleated PP/LCP blends. The fine LCP domains or fibrils act as nucleation sites for the spherulites in the maleated PP/LCP blends. The isothermal

Table V Kinetic Parameters for Nonisothermal Crystallization of m-PP and Its Blends with LCP Calculated for 105°C

m-PP/LCP	T_m (°C)	$T_{1/2}$ (°C)	n	X_c	k ($T_{1/2}$)
100/0	165	107	4	0.43	4.33×10^{-6}
95/5	167	109	3.7	0.45	1.07×10^{-5}
90/10	168	108	3.6	0.46	1.43×10^{-5}
80/20	168	108	3.5	0.47	1.93×10^{-5}
70/30	169	110	3.4	0.45	2.61×10^{-5}
60/40	167	109	3.4	0.48	2.61×10^{-5}

kinetics measurements show that the half-time of crystallization of the m-PP/LCP blends is relatively smaller than that of the maleated PP copolymer. The rate of crystallization is enhanced in maleated PP/LCP blends which exhibit transcrystallinity. Moreover, both isothermal and nonisothermal kinetics measurements reveal that the Ozawa exponents of the PP, m-PP, and PP/LCP blends are identical to the Avrami exponents of these specimens.

This work was supported by a strategic grant (Grant Number 7000-502). S. X. Chen is on leave from the Institute of Chemistry, Academia Sinica, Beijing, China.

REFERENCES

1. G. Kiss, *Polym. Eng. Sci.,* **27,** 410 (1987).
2. L. Minkova, M. Paci, M. Pracella, and P. Magagnini, *Polym. Eng. Sci.,* **32,** 57 (1992).
3. A. M. Sukhadin, A. Datta, and D. G. Baird, *Int. Polym. Process.,* **7,** 218 (1992).
4. D. E. Turek, G. P. Siron, C. Tiu, and O. T. Siang, *Polymer,* **33,** 4322 (1992).
5. F. P. LaMantia, F. Cangialori, U. Pedretti, and A. Roggero, *Eur. Polym. J.,* **39,** 671 (1993).
6. S. S. Bafna, T. Sun, and D. G. Baird, *Polymer,* **34,** 708 (1993).
7. D. Done, A. Sukhadia, A. Datta, and D. G. Baird, *SPE. Tech. Pap.,* **48,** 1857 (1990).
8. B. De Carvalho and R. E. S. Bretas, *J. Appl. Polym. Sci.,* **55,** 233 (1995).
9. S. C. Tjong, S. L. Liu, and R. K. Y. Li, *J. Mater. Sci.,* **30,** 353 (1995).
10. S. C. Tjong, S. L. Liu, and R. K. Y. Li, *J. Mater. Sci.,* **31,** 479 (1996).
11. S. C. Tjong, J. S. Shen, and S. L. Liu, *Polym. Eng. Sci.,* **36,** 797 (1996).
12. R. E. S. Bretas and D. G. Baird, *Polymer,* **24,** 5233 (1992).
13. A. Datta, H. H. Chen, and D. G. Baird, *Polymer,* **34,** 759 (1993).
14. H. J. O'Donnell and D. G. Baird, *Polymer,* **36,** 3113 (1995).
15. G. B. A. Lim and D. R. Lloyd, *Polym. Eng. Sci.,* **33,** 513 (1993).
16. L. Marker, P. M. Hoy, G. P. Tilley, R. M. Early, and O. J. Sweeting, *J. Polym. Sci.,* **38,** 33 (1959).
17. J. Pan, K. Feng, and S. Huang, *J. Zhongshan Univ.,* **3,** 40 (1984).
18. Y. K. Godovsky and S. L. Slonimsky, *J. Polym. Sci. Polym. Phys. Ed.,* **12,** 1053 (1974).
19. G. B. A. Lim and D. R. Lloyd, *Polym. Eng. Sci.,* **33,** 529 (1995).
20. A. Hammami, J. E. Spruiell, and A. K. Mehrotra, *Polym. Eng. Sci.,* **35,** 97 (1995).
21. M. Eder and A. Wlochowicz, *Polymer,* **24,** 1593 (1983).
22. G. B. A. Lim, K. S. Mcguire, and D. R. Lloyd, *Polym. Eng. Sci.,* **33,** 537 (1993).
23. O. Laguna, J. P. Vigo, J. Taranco, J. L. Oteo, and E. P. Collar, *Rev. Plast. Mod.,* **58,** 398 (1989).
24. G. P. Desio and L. Rebenfeld, *J. Appl. Polym. Sci.,* **44,** 1989 (1992).
25. W. Dietz, *Coll. Polym. Sci.,* **259,** 413 (1981).
26. T. Ozawa, *Polymer,* **7,** 1103 (1971).
27. U. R. Evans, *Trans. Faraday Soc.,* **41,** 365 (1945).
28. B. Wunderlich, *Macromolecular Physics,* Academic Press, New York, 1973, Vol. II.